Numerical modeling of FRCM composites for the seismic retrofitting of existing concrete structures

Marco Carlo Rampini, Giulio Zani, Matteo Colombo and Marco di Prisco

Synopsis: Fabric-reinforced cementitious matrix (FRCM) composites are promising structural materials representing the extension of textile reinforced concrete (TRC) technology to repairing applications. Recent experiences have proven the ability of FRCMs to increase the mechanical performances of existing elements, ensuring economic and environmental sustainability. Since FRCM composites are generally employed in the form of thin externally bonded layers, one of the main advantages is the ability to improve the overall energy absorption capacity, weakly impacting the structural dead weights and the structural stiffness and, as a direct consequence, the inertial force distributions activated by seismic events. In the framework of new regulatory initiatives, the paper aims at proposing simplified numerical approaches for the structural design of retrofitting interventions on existing reinforced concrete structures. To this purpose, the research is addressed at two main levels: i) the material level is investigated on the uniaxial tensile response of FRCM composites, modeled by means of well-established numerical approaches; and ii) the macro-scale level is evaluated and modeled on a double edge wedge splitting (DEWS) specimen, consisting of an under-reinforced concrete substrate retrofitted with two outer FRCM composites. This novel experimental technique, originally introduced to investigate the fracture behavior of fiber-reinforced concrete, allows transferring substrate tensile stresses to the retrofitting layers by means of the sole chemo-mechanical adhesion, allowing to investigate the FRCM delamination and cracking phenomena occurring in the notched ligament zone. It is believed that the analysis of the experimental results, assisted by simplified and advanced non-linear numerical approaches, may represent an effective starting point for the derivation of robust design-oriented models.

Keywords: FRCM, retrofitting of concrete structures, tensile behavior, numerical modeling, DEWS test.

INTRODUCTION

Research on Fabric Reinforced Cementitious Matrix (FRCM) composites comprises both the mechanical characterization [1]–[3] and the study of the effectiveness of this technology in upgrading and retrofitting the bearing capacity of reinforced concrete members [4]–[8]. The main advantages of this solution with respect to other retrofitting techniques are the better compatibility with irregular surfaces (such as concrete substrates), the easier workability, the higher durability and the smaller cost of installation [9].
Finite element analyses on FRCM-strengthened elements represent an important tool to predict the enhancement of their structural capacity [10], [11]. The aim of this study is not only to verify the effectiveness of FRCM composites in strengthening and retrofitting reinforced concrete elements, but also to assess the potential of available numerical approaches in simulating the behavior of these materials when applied as externally bonded reinforcements. Following the tensile characterization of the chosen system (comprising both the embedded alkali-resistant (AR) glass fabric and the cement-based composite), three different numerical models were implemented using the commercial software Abaqus 6.14-5, in order to propose several ways to reproduce the behavior of such materials. The comparison of the simulations results with the experimental behaviors allowed to identify the best approach to be used also at the macro-scale level, through Double Edge Wedge Splitting specimens.
In the end, the experimental behavior at the macro-scale level was compared to the numerical results, considering the presence or the absence of a pre-damage and alternative orientations of the fabric reinforcement.

EXPERIMENTAL INVESTIGATION AND DISCUSSION OF THE RESULTS

The first part of the experimental campaign described in this section is focused on the mechanical characterization of the base materials used to manufacture different specimens. Compression and indirect tensile tests were performed to obtain the mechanical properties of the substrate concrete and of the pre-mixed retrofitting mortar, while the inner AR-glass textile was characterized by means of a series of uniaxial tensile tests. In the following phase, the tensile behavior of the chosen FRCM system was investigated and Double Edge Wedge Splitting (DEWS) tests were performed to assess the effectiveness of the externally-bonded reinforcing technique.

Materials

Substrate concrete

The mix design of the concrete used for the DEWS substrate specimens is presented in **Table 1**. The resulting matrix is characterized by a water to binder ratio equal to 0.41 and a water to cement ratio of 0.66. Mechanical properties of the substrate concrete are obtained by means of compression and Brazilian tests. Compression tests were performed on eight nominally identical cube specimens (100 mm (3.94 in.) in size), while the dimensions of the indirect tensile ones are 100 × 100 × 50 mm^3 (3.94 × 3.94 × 1.97 $in.^3$). The results of the mechanical characterization are summarized in **Tables 2-3**; the average cylindrical compressive strength, f_{cc}, evaluated as 0.83 times the cubic one, and the Brazilian tensile strength, $f_{ct,sp}$, are respectively equal to 46.69 MPa (6,771.21 psi) and 2.89 MPa (419.44 psi). Upon the suggestion of Model Code 2010 [12], a coefficient between the tensile and the Brazilian strengths equal to 1.00 and a Young's modulus of 35.93 GPa (5,211.60 kpsi) will be adopted in the following numerical simulations.

Table 1–Substrate concrete composition

Component	Dosage [kg/m^3 (lb/ft^3)]
Cement I 52.5	250 (15.61)
Sand 0-3 mm	620 (38.70)
Sand 0-12 mm	540 (33.71)
Gravel 8-15 mm	610 (38.08)
Water	165 (10.30)
Superplasticizer	4÷4.5 (0.25 ÷ 0.28)
Calcareous filler	150 (9.36)

Table 2–Cylindrical compressive strengths of the pre-mixed mortar: individual values, average values, standard deviation and percent coefficient of variation.

Specimen	f_{cc} [MPa (psi)]
N1	44.07 (6,392.03)
N2	48.26 (6,998.72)
N3	50.02 (7,255.13)
N4	50.69 (7,351.43)

N5	39.92 (5,790.14)
N6	40.99 (5,945.42)
N7	48.04 (6,967.43)
N8	51.50 (7,469.40)
Average	46.69 (6,771.21)
std	4.47 (647.72)
%CV	9.57 %

Table 3–Brazilian tensile strengths of the pre-mixed mortar: individual values, average values, standard deviation and percent coefficient of variation.

Specimen	f_{ctb} [MPa (psi)]
N1	2.81 (407.68)
N2	3.32 (481.67)
N3	2.82 (408.33)
N4	3.44 (499.51)
N5	2.65 (384.89)
N6	2.31 (334.54)
Average	2.89 (419.44)
std	0.42 (61.56)
%CV	14.5 %

Substrate steel reinforcement

Each DEWS specimen was reinforced with a steel welded mesh made by ϕ6 mm (0.236 in.) B450A grade deformed bars. The grid was positioned in the central section of the specimen, as shown in **Fig. 3a**; please note that three bars run in the horizontal direction. The numerical constitutive law (yield strength and ultimate strain) used in the non-linear simulations was calibrated as explained in the numerical section, while the elastic modulus was taken equal to 210.00 GPa (30,456.85 kpsi).

Pre-mixed retrofitting mortar

The FRCM system consisted of a commercial shrinkage-compensated thixotropic repair mortar, suitable for retrofitting applications of concrete structures. The composition of the cementitious pre-mixed mortar is displayed in **Table 4**.

Table 4–Pre-mixed mortar composition

Component	Dosage [kg/m^3 (lb/ft^3)]
Ready-mix admixture	1,840 (114.86)
Water	276 (17.23)
Expansive agent	18.4 (1.15)

The results of bending and compressive tests, performed on six nominally identical 40 × 40 × 160 mm^3 (1.57 × 1.57 × 6.30 in.^{3}) specimens, following the UNI EN 196 prescriptions [13], are summarized in **Table 5**. The tensile strengths were computed using the following formula, in accordance with Model Code 2010 [12]:

$$f_{ct}=f_{ctf}\frac{\alpha\cdot h^{0.7}}{1+\alpha\cdot h^{0.7}},$$

where h is 40 mm (1.57 in.) and α is taken equal to 0.06. Mean cubic compressive strength, $f_{cc,avg}$, and mean flexural tensile strength, $f_{ctf,avg}$, are equal to 58.94 MPa (8,548.02 psi) and 7.02 MPa (1,017.76 psi), respectively. The elastic modulus is taken equal to 28.00 GPa (4,060.91 kpsi), as declared by the manufacturer.

Table 5–Bending, tensile and compressive strengths of pre-mixed mortar: discrete values, average values, standard deviations and shape m coefficient of the two-parameter Weibull distribution.

Specimen	f_{ctf} [MPa (psi)]	f_{ct} [MPa (psi)]	f_{cc} [MPa (psi)]
N1	8.26 (1198.24)	3.66 (530.17)	69.08 (10018.26)
N2	7.15 (1036.36)	3.16 (458.54)	65.20 (9456.81)
N3	8.46 (1226.39)	3.74 (542.62)	59.94 (8692.90)
N4	7.28 (1056.30)	3.22 (467.37)	56.77 (8233.37)

N5	5.11 (741.14)	2.26 (327.92)	49.52 (7182.46)
N6	5.85 (848.16)	2.59 (375.92)	53.12 (7704.30)
Average	7.02 (1017.76)	3.10 (450.32)	58.94 (8548.02)
std	1.32 (191.42)	-	7.35 (1066.22)
std %	19 %	-	12 %
m (Weibull)	7.15	-	-

AR-glass fabric

A double leno weave alkali-resistant glass fabric, impregnated with an epoxy resin, was chosen as the reinforcement of the FRCM retrofitting system. The geometrical and mechanical characteristics, obtained from five uniaxial tensile tests on 70 mm (2.76 in.) wide strips, following the ISO 4606 procedure [14], are displayed in **Table 6**. The fabric efficiency parameter, EF_f according to [1], was evaluated in both the warp and the weft directions and represents information regarding the material utilization rate.

Table 6–Alkali-resistant glass fabric characteristics *(*average of four samples)*

Characteristic	warp	weft
Wire spacing [mm (in.)]	38 (1.496)	38 (1.496)
Roving fineness [Tex]	2 × 2400	4 × 2400
Filament diameter [μm]	27	27
Eq. thickness [mm (in.)]	0.093 (0.0037)	0.093 (0.0037)
$P_{max,avg}$ [kN (lb)]	12.50 (2,810.25)*	11.70 (2,630.40)
Fabric efficiency EF_f	0.87	0.82

FRCM tensile characterization

Six geometrically identical FRCM samples were manufactured using the pre-mixed mortar and the AR-glass fabric described before. They were cast by means of a traditional hand lay-up technique, placing one layer of textile at mid-thickness of each specimen (three in the warp and three in the weft directions). During the first day of the curing phase, a plastic foil was applied on the formworks, then the samples were cured at laboratory conditions.

The results of the uniaxial tensile tests, performed at a constant stroke rate of 20 μm/s on the FRCM specimens, 70 × 400 × 10 mm^3 (2.76 × 15.75 × 0.39 in.^{3}) in size, in both the warp and the weft directions, are depicted in terms of nominal stress vs. normalized displacement (**Fig. 1**) and nominal stress vs. average strain (**Fig. 2**). The normalized displacements were computed dividing the stroke measurements (cross-head displacement) by the free specimen length, equal to 300 mm (11.81 in.), while the average strains were evaluated as the ratio between the integral crack opening displacements (COD) and the gauge length of about 200 mm (7.87 in.). The COD is the average between the two measurements read by two linear variable differential transformers (LVDT) placed on the opposite faces of each sample. The nominal FRCM stresses, σ_{FRCM}, were computed dividing the experimental load by the measured cross-section; the average thickness was equal to 10.86 mm (0.43 in.) for the warp samples and 10.53 mm (0.41 in.) for the weft ones. Please note that, in **Fig. 1**, when one of the experimental responses was lost, the vertical mean curve was still computed considering the remaining specimens, while the maximum mean stress values, 11.92 MPa (1,728.79 psi) for the warp and 9.43 MPa (1,367.66 psi) for the weft directions, are obtained averaging the three peaks. The efficiency of the composite solution is usually computed from the test results as the ratio between the capacity of the composite divided by the one of the plain textile, in terms of load. For this FRCM system the efficiency parameters, EF_{FRCM} [1], [15], are equal to 0.73 and 0.60, respectively in the warp and in the weft directions.

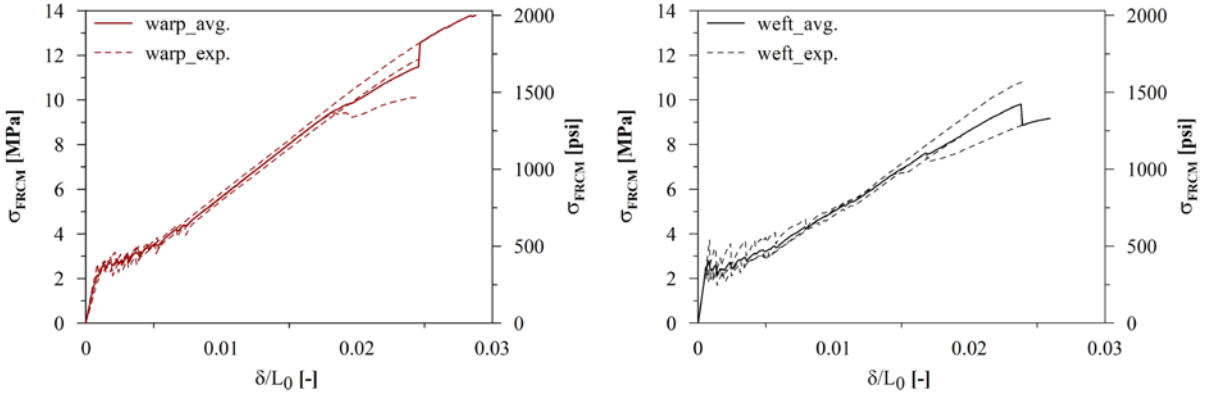

(a) (b)

Fig. 1–Average tensile responses of the FRCM system in terms of nominal stress vs. normalized displacement in the warp (a) and in the weft directions (b).

A well-established analytical model [1], [16], [17] was used to predict the tensile behavior of the FRCM system both in the warp and the weft directions, cutting the responses by using the experimentally evaluated efficiency parameters (EF_f and EF_{FRCM}). From the comparison with the experimental responses, shown in **Fig. 2**, it is possible to notice the good level of approximation reached. Due to this reason, these curves may be effectively used as simplified constitutive laws for the FRCM material.

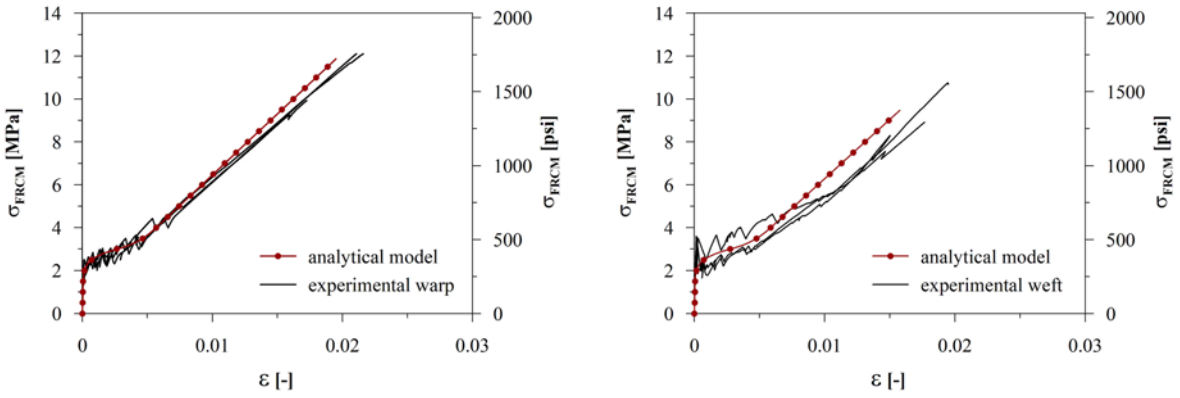

(a) (b)

Fig. 2– Comparison between the predicted analytical curves [1] and the experimental responses in terms of normalized stress vs. strain in the warp (a) and in the weft directions (b).

Double Edge Wedge Splitting (DEWS) tests

The Double Edge Wedge Splitting test (DEWS) [18] is an indirect tensile test developed as an extension of the Wedge Splitting (WS) test [19]. The main difference between this and other indirect tests (i.e. Brazilian and bending tests) is the ability of the DEWS to uncouple tensile and compressive stresses along the critical region. Due to the inclination at 45° of the faces over which the load is applied, see **Fig. 3**, the formation of two compressive arches occurs, inducing a mode I tension stress distribution on the middle section, called ligament [18]. Thanks to this, DEWS tests are suitable to assess the effectiveness of FRCM strengthening and retrofitting interventions. In fact, as in the real reinforced members, external loads are applied directly to the structure and stresses are transferred to the FRCM reinforcement layers by means of chemo-mechanical adhesion between the repair mortar and the substrate [15], [20]. Moreover, the two composite layers are subjected to a quasi-uniform distribution of tensile stresses.

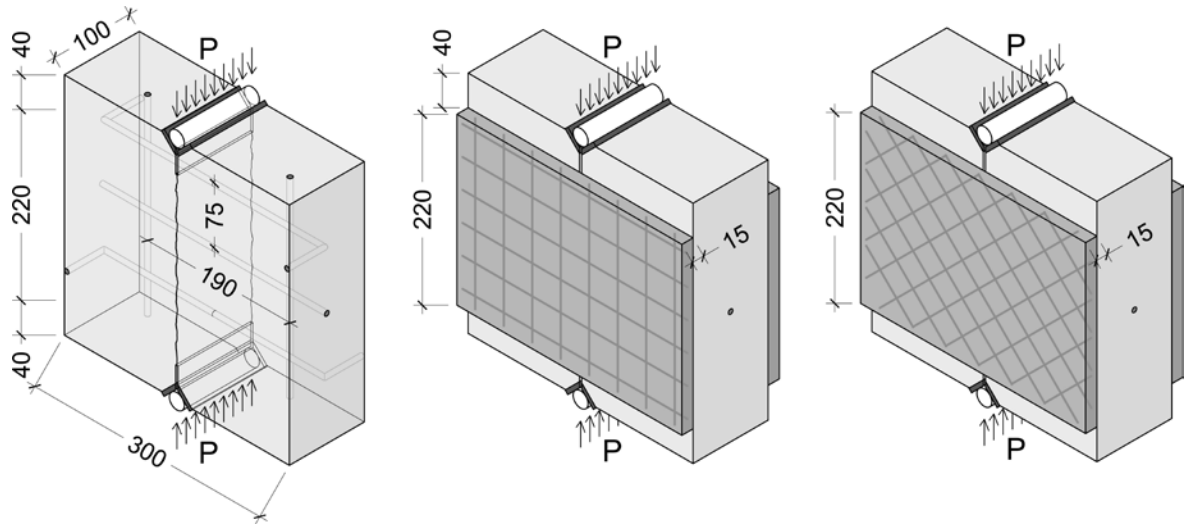

(a) (b) (c)

Fig. 3– Double Edge Wedge Splitting test setup in the pre-cracking phase (a) and post-reinforced one, with different orientation of the inner fabric: warp (b) and 45° (c) [dimensions expressed in mm, 1 mm = 0.039 in.]

Eight nominally identical specimens (dimensions are displayed in **Fig. 3a**) were cast with the concrete previously described. Four 5 mm (0.20 in.) thick steel plates were glued to the inclined notched faces and two ϕ20 mm (0.79 in.) steel cylinders were used to uniformly distribute the vertical load. The friction between the steel plates and the loading cylinders affects, through a tangential force, the transverse tensile load within the ligament. In order to minimize this effect, a graphite paste was applied between the steel surfaces as a lubricant. The ratio between the transverse splitting force F_{SP} and the vertical load P applied by the actuator was experimentally computed on a specifically designed specimen instrumented with a transverse load cell and resulted equal to $F_{SP}/P = 0.76$. This value depends on both the specimen and the notch dimensions and the friction coefficients of the loading surfaces (steel cylinders to steel plates and steel plates to concrete specimen).

Pre-cracking of the substrate samples

After the curing period: i) two specimens were tested up to failure, providing reference responses (REF), **Fig. 4a**; ii) four were pre-cracked (PRE) at a level of crack opening, COD, equal to 1.5 mm (0.06 in.), **Fig. 4b**, to simulate a cracked condition of the substrate before the retrofitting; and iii) the remaining two specimens were kept non-damaged (ND). Two LVDTs were placed at the center of the two opposite faces of each specimen to record the evolution of the crack opening during the test. In **Fig. 4**, the experimental curves in terms of splitting force (F_{SP}) vs. average COD are shown. The average values of both the maximum and the cracking splitting forces are displayed on the graphs.

Pre-cracking tests were performed by using a hydraulic actuator and controlling the load increase at a constant rate of 60 N/s (13.49 lb/s) up to 15 kN (3,372.30 lb), then controlling the stroke at 1.67 μm/s. A summary of the different pre-cracking tests is reported in **Table 6**. Please note that the PRE tests were stopped as one of the crack opening measurements reached the desired value. Due to the intrinsic asymmetry of the responses, the average COD does not reach 1.5 mm (0.59 in.) in each sample, **Fig. 4b**. The average values of the maximum splitting force, equal to 45.69 kN (10,272 lb), and the ultimate COD reached during the REF tests, 3.66 mm (0.14 in.), were used to calibrate the constitutive law of the steel reinforcement. It is also interesting to observe that after the formation of the crack in the ligament zone, a decrease of the sustained load occurred due to the transfer of the splitting force, initially sustained by the concrete, to the transverse steel rebar. In these tests, the sudden reduction is also caused by an insufficient test control related to the use of a hydraulic actuator. The results suggest that, following the propagation of the ligament crack, complete debonding of the three transverse bars occurred.

Table 6–Summary of pre-cracking DEWS tests

Specimens	nr.	Test end
Non-damaged (ND)	2	not tested
Pre-cracked (PRE)	4	COD =1.5 mm (0.59 in.)
References (REF)	2	failure

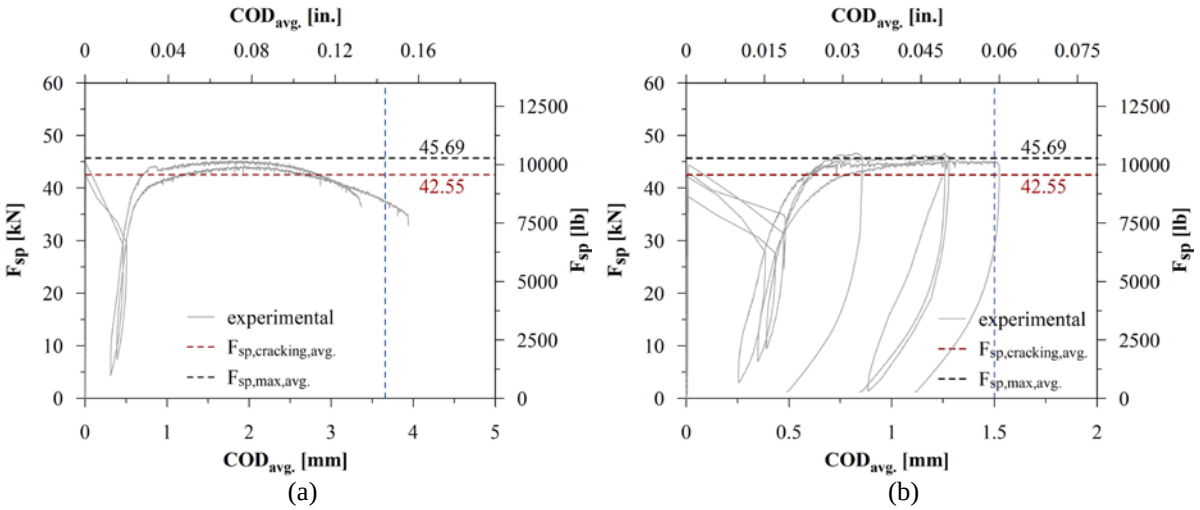

Fig. 4– Experimental responses in the pre-cracking phase in terms of splitting force vs. average crack opening displacement for reference (a) and pre-cracked at COD=1.5 mm specimens (b). Average splitting force values refer to all the specimens.

Test on strengthened and retrofitted specimens

After the first series of tests, the non-damaged (ND) and pre-cracked (PRE) specimens were strengthened/retrofitted by the application on both sides of a 15 mm (0.59 in.) thick layer (**Figs. 3b-c**) of the

FRCM system previously introduced. Before the application of the externally bonded reinforcement, the substrate was properly prepared by means of a hydro-scarification with a pressure of around 1,800 atm. The FRCM layers were applied with different orientations of the embedded fabric (0° and 45° between the warp and the horizontal direction). Six post-reinforced DEWS tests on reinforced specimens were carried out with the same control and rate used in the pre-cracking phase; a summary is displayed in **Table 7**.

Table 7–Summary of DEWS tests after the FRCM application

Specimens	nr.	fabric orientation
Non-damaged (ND)	2	0° - warp
Pre-cracked (PRE)	2	0° - warp
Pre-cracked (PRE)	2	45°

From the experimental results shown in **Figs. 5-6**, it is possible to notice the increased ultimate capacity associated with the FRCM application. The mean peak values of the splitting force are 95.97 kN (21,575.99 lb), for the specimens with the fabric applied with the warp direction perpendicular to the ligament crack, and 76.28 kN (17,149.28 lb), for the ones with the fabric oriented at 45° (respectively 2.1 and 1.7 times the ultimate splitting force of reference specimens). Some of the experimental curves are represented with dashed lines; this means that they represent the envelopes of noisy experimental responses, affected by an imperfect test control. It is important to underline that, thanks to the hydro-scarification of the substrate, no delamination between the mortar and the concrete surface was observed at the end of each test. Multiple cracks occurred in the FRCM layer, starting from the middle of the specimen (ligament zone) and propagating through the composite thickness (see the top view in **Fig. 17c**).

Comparing the responses of the warp-retrofitted specimens, **Fig. 6a**, it is worth to notice that the influence of the pre-damage appears negligible. In fact, no great differences between the peak values of the splitting force and of the ultimate crack opening are highlighted. In case of PRE specimens, in addition to the above-mentioned effect on the peak splitting forces, it can be noticed that a different orientation of the textile also influences the ductility, **Fig. 6b**. The ultimate crack opening is larger in the case of 45° oriented fabrics, probably due to better controlled delamination at the mortar-fabric interface in the warp-reinforced DEWS specimens. In comparing the results, it should be noted that the lack of anchorage of some edge yarns in the 45° configuration may result in a slightly different failure mode (local fiber sliding also occured).

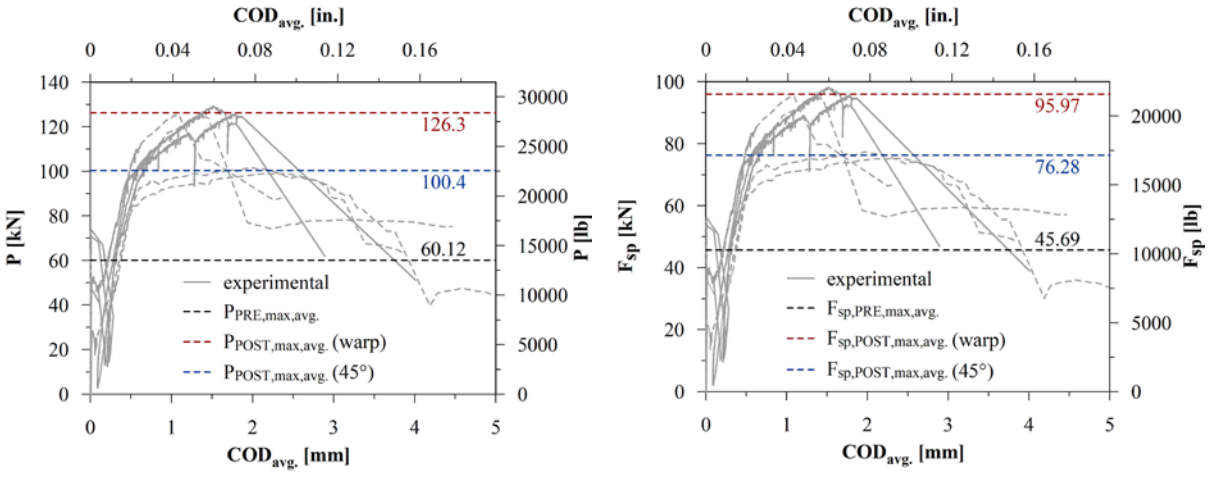

Fig. 5– Experimental responses in the post-reinforced phase in terms of vertical load (a) and splitting force (b) vs. average crack opening displacement

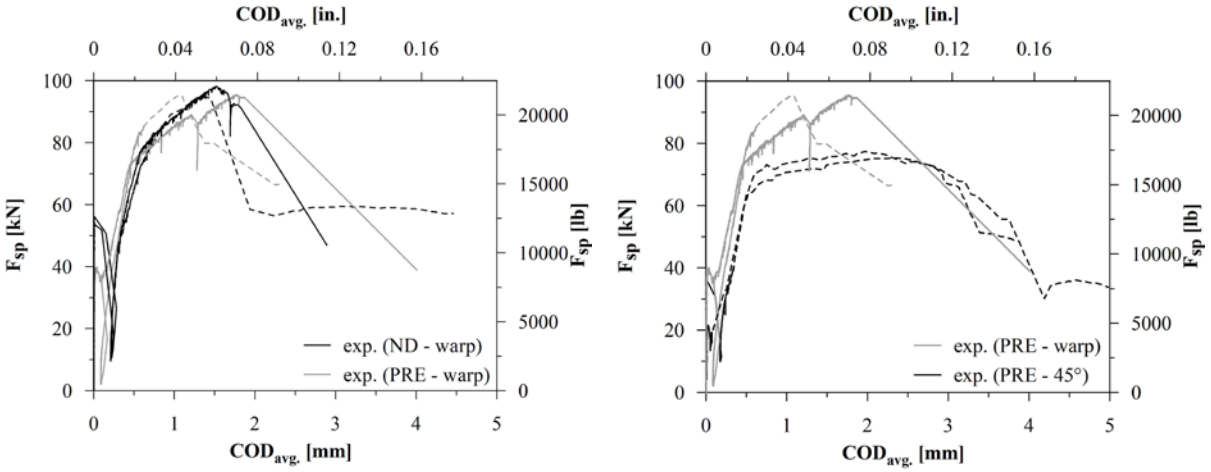

(a) (b)

Fig. 6– Comparison between the experimental responses in terms of splitting force vs. average crack opening displacement for warp reinforced (a) and pre-cracked specimens (b).

Moreover, it is possible to observe that the collapse was always governed by the textile rupture, while the yielding of the transverse rebar took place at around 90-100 kN (20,233.80-22,482 lb) of vertical load *P*. These observations were confirmed by the non-linear finite element analysis described in the following.
Referring to Fig. 7, it is possible to observe that the difference between the two average first cracking F_{sp} recorded in the ND and PRE specimens (54.89 kN – 42.55 kN) is smaller than the one exhibited by the PRE-warp specimens (39.64 kN), on the contrary of what expected (the difference was expected to be associated to the sole FRCM capacity). Full explaination of this is still under investigation, even though this might be related to non-uniform stress distributions along the ligament (in the PRE-warp the effect of the notch vanishes due to the presence of a passing crack in the substrate and the tensile capacity of the FRCM is fully exploited). Please note that, in all the cases, due to the hydro-scarification the thickness of the retrofitting layers increases (the thickness of a single FRCM layer can reach about 30 mm, to be compared to the nominal 15 mm).

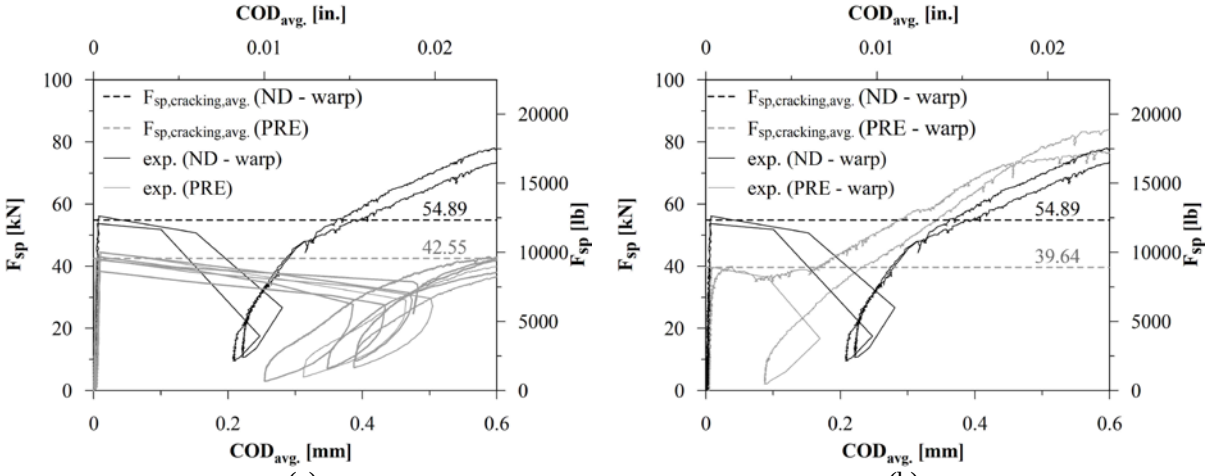

(a) (b)

Fig. 7– Comparison between the experimental responses of the ND with the PRE specimens (a) and of the ND with the PRE-warp ones (b), in terms of splitting force vs. average crack opening displacement.

NUMERICAL MODELLING AND DISCUSSION OF THE RESULTS

In this section, the aim is to simulate the experimental responses of the composites, both at the material and the meso-scale level, by means of non-linear numerical analyses.
In the first part, different material models were calibrated to simulate the uniaxial tensile behavior of the chosen FRCM system, underlining the pros and cons of each approach. Then, one of the presented models was chosen to model the FRCM behavior, when applied as reinforcement of DEWS samples.
Both the numerical analyses were performed by making use of the commercial code Abaqus 6.14-5, following an engineering-oriented procedure in order to simplify the simulation of the FRCM reinforcement.

Modeling of the FRCM uniaxial tensile tests

3D continuum shell elements were chosen for the finite element simulation of the FRCM behavior under tensile action. The constitutive material modeling was performed in three different ways, in ascending order of complexity. In the first one, model "A", the material was considered as homogeneous and the analytical curves shown in **Fig. 2** were used as tensile constitutive laws. In this approach, the post-elastic behavior was described by a stress-strain relation, using the concrete damaged plasticity (CDP) model [21] implemented in Abaqus. In the second case, model "B", a rebar layer was defined by embedding a set of surface elements in the continuum shell [22]. This assumption results in an over-estimation of the number of localizations (cracks) in the numerical simulation, due to the lack of a proper bond-slip law and the absence of the geometrical defects introduced by the yarns orthogonal to the loading direction. Each set represents one of the two main directions of the plain fabric, while the mortar properties were assigned through the CDP, using a mode I fracture energy (G_f) approach in the post-elastic phase. The average value of the tensile strength was used and, in order to effectively simulate the brittleness of the cracking process in the matrix and to control the amount of numerical energy dissipation, the G_f value was set to 20% of the one computed from the mean compressive strength according to Model Code 2010.

The need to increase the matrix brittleness appears to be justified by two main reasons: i) a rigid bond between the fabric and the matrix is assumed in the numerical model, even though a non-linear bond-slip law was observed by many researchers; ii) the adopted Model Code 2010 formulation, conceived for concrete, may not be satisfactorly applicable to the employed thixotropic mortar, due to the presence of a significant porosity.

The same approach was used in model "C", the only two differences being: i) the choice to randomly assign, to each strip, **Fig. 8**, diverse values of tensile strength; and ii) the fact that the post-elastic material law was directly defined in terms of stress-strain, to guarantee a proper fracture energy regularization. The set of tensile strengths used in model "C" was based on a two-parameter Weibull function, computed by means of the experimental results in **Table 5**. This distribution is the same used in the stochastic cracking model implemented before. In both models "B" and "C", the warp and the weft layers were defined as elastic up to failure; in each direction, the ultimate fabric capacity, σ_f, and the elastic modulus, E_f, were computed by multiplying the manufacturer data, respectively 2,000 MPa (290,065.27 psi) and 70 GPa (10,152,284.26 psi), by the fabric efficiency EF_f [1].

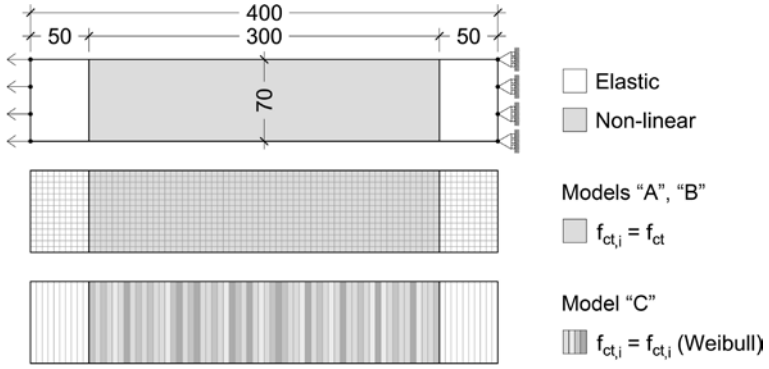

Fig. 8– Numerical model representation: boundary and mesh discretization for all the different models of FRCM samples.

In all the models, the boundary/load conditions were the ones displayed in **Fig. 8**. The constitutive law in compression was defined as elastic-plastic with Young's modulus and mean compressive strength taken from the experimental characterization, while the Poisson's ratio was set equal to 0.2. To reduce numerical stress concentration at the ends, two lateral 50 mm (1.97 in.) long zones were modeled as indefinitely elastic and the non-linear behavior of the material was only assigned to the central 300 mm (11.81 in.) long area.

A square mesh grid of 5 mm (0.20 in.) side was used for both models "A" and "B", while strip-shaped elements were used in model "C". In all cases, the assigned elements were linear quadrilateral (type S4R) and five points of integration were adopted through the thickness. The concrete damaged plasticity parameters were set to the default ones (dilation angle of 38°, eccentricity of 0.1, f_{b0}/f_{c0} of 1.16 and K of 0.67), except for the viscosity parameter, which was fixed at 1E-006, in favor of the analysis stability [23].

Comparison between different modeling results

As expected, a good correlation between the experimental tensile test responses and the numerical curves obtained by performing a non-linear numerical analysis with the assumptions of model "A" was achieved, **Fig. 9**. Despite the simplicity of this model implementation, it is important to underline that, due to the intrinsic isotropy of this numerical approach, it is not possible to simulate the tensile behavior in a direction different from alternatively the warp and the weft ones.

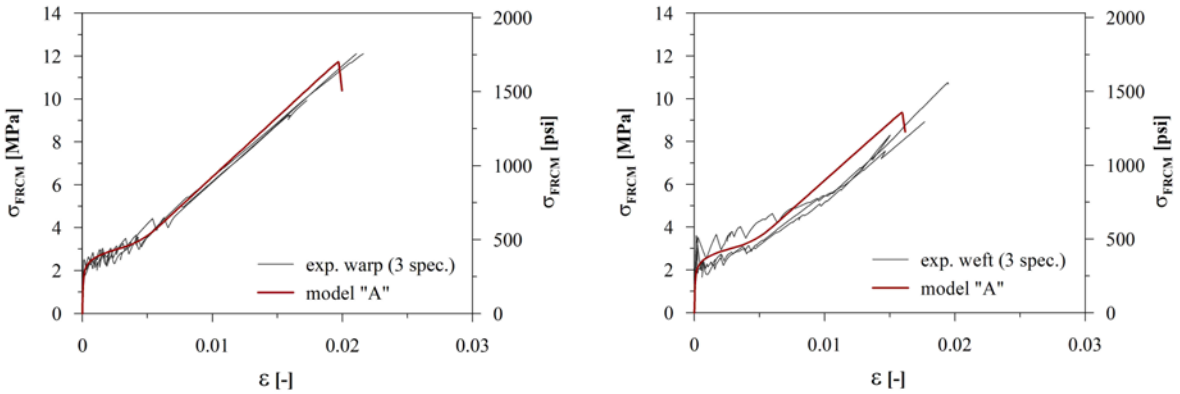

(a) (b)

Fig. 9– Comparison between the numerical results for model “A” and the experimental responses both in the warp (a) and in the weft (b) directions.

The main advantage of model “B” is the possibility to define an orthotropic material, with two or even more rebar layers that represent the fabric directions. Regarding the comparison with the experimental responses, **Fig. 10**, it is interesting to notice the typical loss and recovery of stress during the multi-cracking branch of the curve, caused by the brittleness of the matrix and the transfer of the internal forces to the equivalent rebar layers. Pertaining to the ultimate stress values reached in the numerical simulations, the over-estimation of the capacity is related to the properties assigned to the inner fabric. In fact, glass rovings were modeled elastic up to the fabric ultimate stresses, without applying any composite efficiency parameter, EF_{FRCM}.

In addition to the same observations done for model “B”, in the case of model “C” it is possible to notice that the slope of the second branch is adequately reproduced, **Fig. 11**, and a better estimation of the strain at which the third branch starts is obtained, **Fig. 12**.

In **Fig. 13**, the equivalent plastic strains distribution of each model is displayed, at different levels of deformation. It can be noticed that, only in the case of model “C”, the plastic strain evolution properly represents the typical cracking pattern on an FRCM composite under tension. This is due to the random assignment of different tensile strengths to each strip.

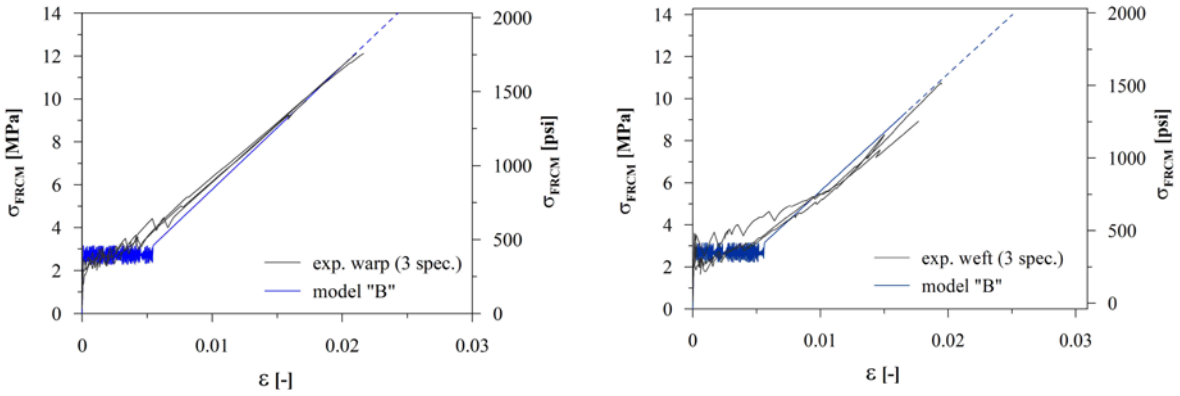

(a) (b)

Fig. 10– Comparison between the numerical results for model “B” and the experimental responses both in the warp (a) and in the weft (b) directions.

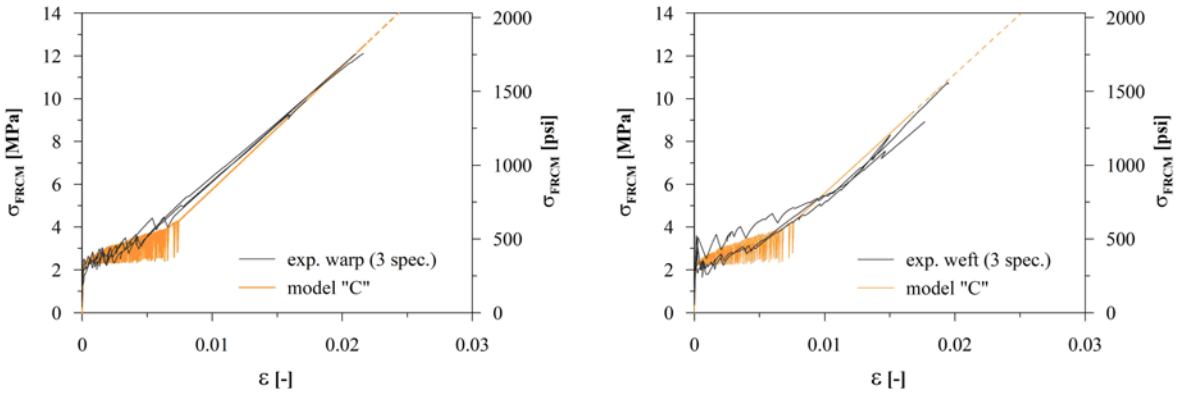

(a) (b)

Fig. 11– Comparison between the numerical results for model "C" and the experimental responses both in the warp (a) and in the weft (b) directions.

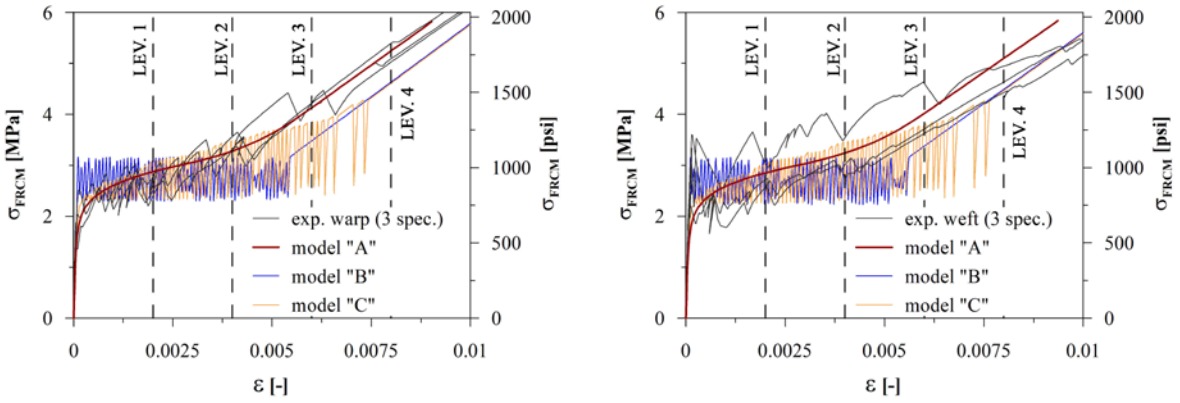

(a) (b)

Fig. 12– Comparison between the numerical and experimental curves up to the end of the second branch of the mechanical response in tension.

Fig. 13– In-plane principal plastic strain distribution at increasing steps (LEV.1-4) of the numerical simulations for each material model adopted.

Modeling of the DEWS tests

A 3D model was developed to numerically simulate the DEWS responses, both in the pre-cracking and in the post-reinforced phases. A schematization of the numerical model is displayed in **Fig. 14a**. The bottom cylinder was hinged and its rotation was not allowed, while the vertical displacement of the upper one, as in the experimental test, increased in time. An important aspect of the modeling was the choice of both the cylinder-plates and the plates-concrete contact properties. A hard contact in the normal direction and tangential behaviors with friction coefficients respectively equal to 0.11 and 0.5 were chosen. Only half of the specimen was modeled, exploiting the nominal geometrical symmetry.

From the experimental evidence of both the pre-cracking and post-reinforced phases, it was observed that outside the central zone the behavior of the materials basically remained elastic. Due to this reason, the substrate concrete

was considered elastic in the external zones, in order to simplify the numerical computation, **Fig. 14b**. In the central part (grey solid hatch), the compression constitutive law was computed in accordance with Model Code 2010 from the experimental characterization results, while the inelastic tensile behavior was implemented in terms of fracture energy. A reduction of the G_f (20% of the total one) was again assigned to the ligament elements, to favour strain localization. Poisson's ratio was set equal to 0.2 and the same CDP parameters were adopted.
The substrate was modeled with linear hexahedron (C3D8R) elements with different sizes: 2 mm (0.08 in.) in the ligament zone and 10 mm (0.39 in.) in the rest of the model. Under the steel plates, linear tetrahedron (C3D4) elements were used, in order to improve the mesh quality.
The FRCM layer was simulated according to the procedure previously introduced as model "B". This choice was done because of the possibility to account for the material orthotropic behavior. Due to the narrowness of the process zone, it was decided to neglect the Weibull distribution of tensile strengths and therefore no simulations with model (C) were carried out.
Regarding the FRCM mesh sizes, 5 mm (0.20 in.) linear quadrilateral (S4R) elements were used in the process zone and size increases towards the external regions, up to 20 mm (0.79 in.). The FRCM layers were attached to the substrate surface preventing any differential slippage between the reinforcing layer and the solid specimen.

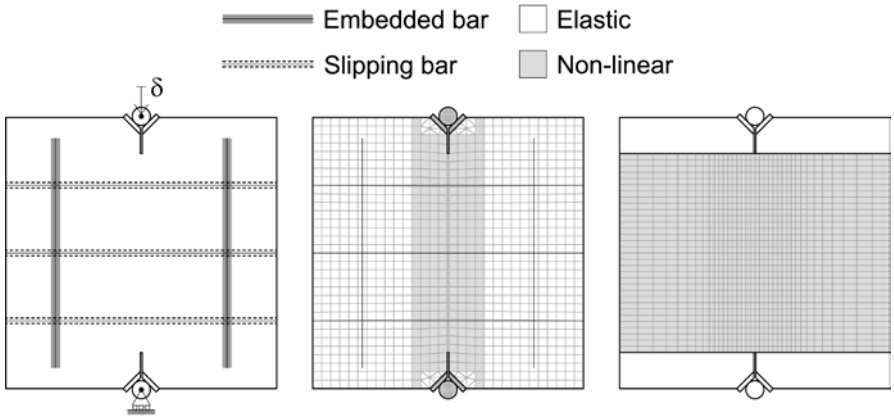

Fig. 14– Numerical model representation: boundary and constraints (a), mesh discretization for the concrete substrate (b) and the reinforcement FRCM layer (c).

Pre-cracking numerical modeling
In absence of a full mechanical characterization of the steel bars, their constitutive law was preliminary calibrated, in order to better approximate the experimental response in the pre-cracking phase of the DEWS tests. In particular, the yield strength was evaluated assuming that, at the peak of the curve, the splitting force is uniformly distributed among the three transverse bars, while the ultimate strain was set so as to ensure the same crack opening displacement at failure in the numerical and the experimental responses, **Fig. 15**. The chosen simplified constitutive law is considered acceptable, because in the reinforced DEWS tests the rebar failure takes place after the rupture of the textile, **Fig. 5**. As shown in **Fig. 14a**, only the vertical rebars were embedded in the concrete sample, while the transverse ones were left free to slip at zero bond stress. This assumption seems to be adequate to simulate the tests, being confirmed by the previous experimental observation (see Section "*Pre-cracking of the substrate samples*"). The result of the pre-cracking numerical simulation is displayed in **Fig. 15**.

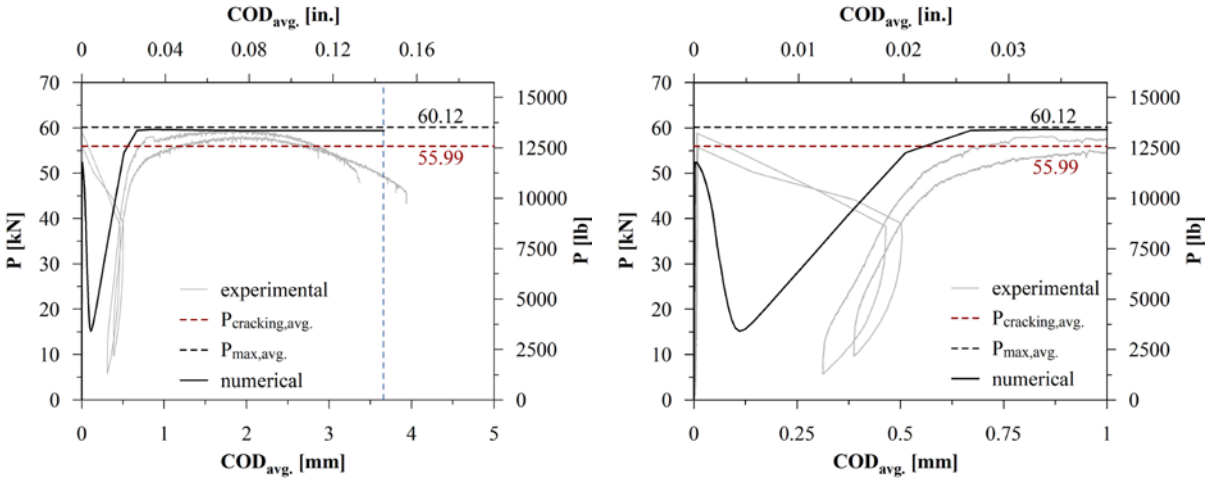

Fig. 15– Comparison between the experimental and the numerical results for the reference (REF) specimens: global curves (a) and detail in the COD range 0-1 mm (b).

Post-reinforced numerical modeling

Three different models were developed to simulate the experimental behaviors after the application of the FRCM layers. The first one represents the response of the non-damaged (ND) specimens, directly strengthened with the composite. The results obtained are displayed in **Fig. 16**. It is possible to notice the ability of the model to catch: i) the stiffness of the experimental response during the re-loading phase, following the ligament cracking; and ii) the extension of the non-linear process zone. In fact, in **Fig. 17**, it can be noticed that the plastic strain distribution adequately represents the damaged zone both on the substrate concrete and on the composite layer. In particular, focusing on the substrate concrete, the damage probably occurred due to the lack of a bond-slip law describing the slippage of the AR-glass fabric within the surrounding mortar (inter-laminar delamination). In fact, FRCM composites generally exhibit a good bond with the concrete substrate and failure tends to occur at the fabric-matrix interface [5].

The other two models represent the simulation of the experimental tests on pre-cracked specimens (PRE). To simulate the presence of the 1.5 mm (0.06 in.) wide crack, it was decided to remove all the substrate elements in the ligament zone. The modeling of the attached FRCM layers was done following the same procedure described previously but, thanks to the orthotropic behavior of the model used to simulate the composite, it was also possible to assign the correct orientation at 45° of the pre-cracked DEWS reinforced with an inclined fabric.

The numerical results, displayed in **Fig. 18-19**, show the ability to catch the experimental behaviors with a satisfactory degree of accuracy, as in the ND model. At this stage of the research, all the numerical simulations stop in proximity of the yielding of the horizontal steel bars and the reason of this numerical problem, probably caused by the absence of a bond-slip law in the FRCM model, which results in a severe strain localization in the embedded fabric.

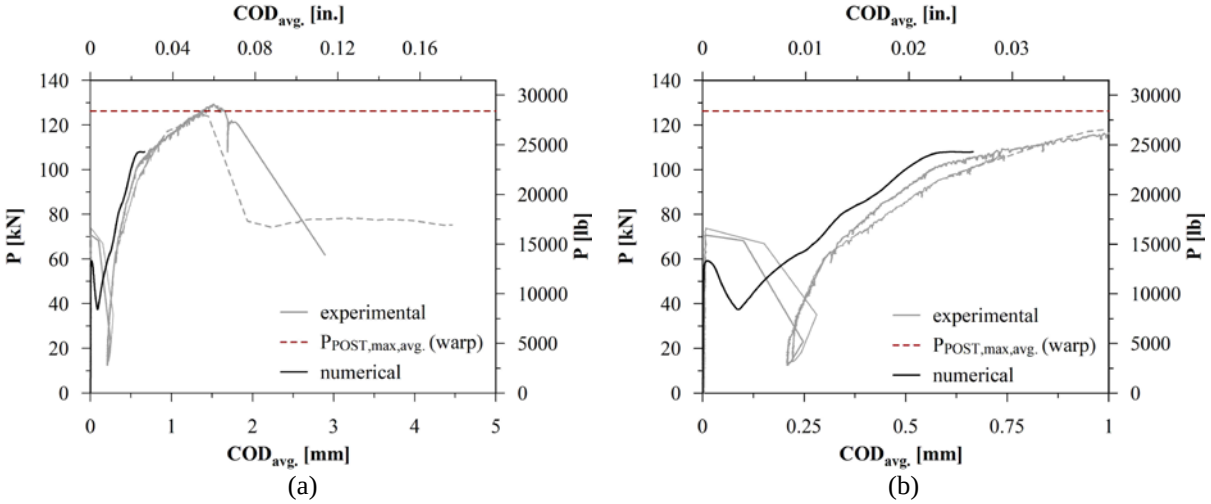

Fig. 16– Comparison between the experimental and the numerical results for the non-damage (ND) specimens strengthened with warp-oriented FRCM: global curves (a) and detail in the COD range 0-1 mm (b).

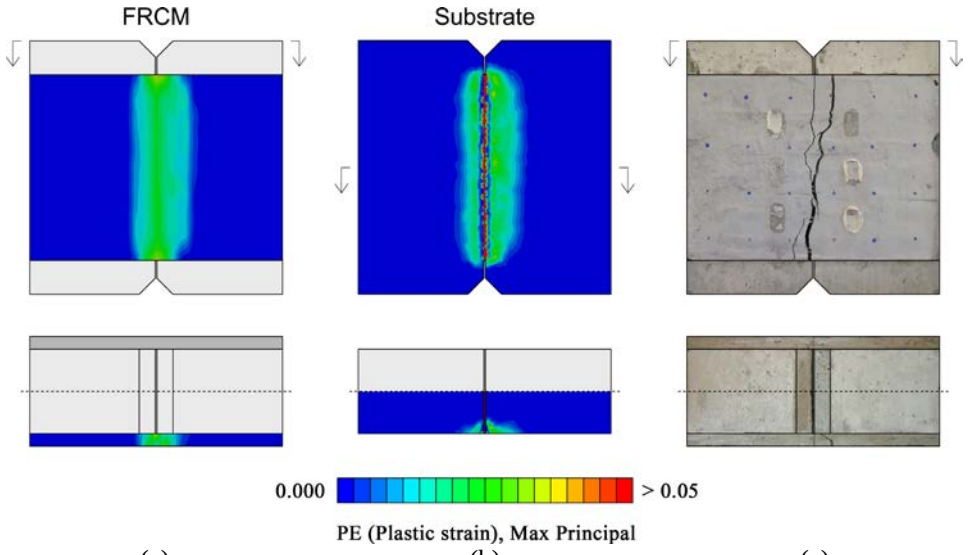

(a) (b) (c)

Fig. 17– Comparison between the in-plane plastic strain numerically evaluated (a-b) and the crack pattern distribution at the end of the experimental test (c), for the non-damaged (ND) specimens strengthened with warp-oriented FRCM.

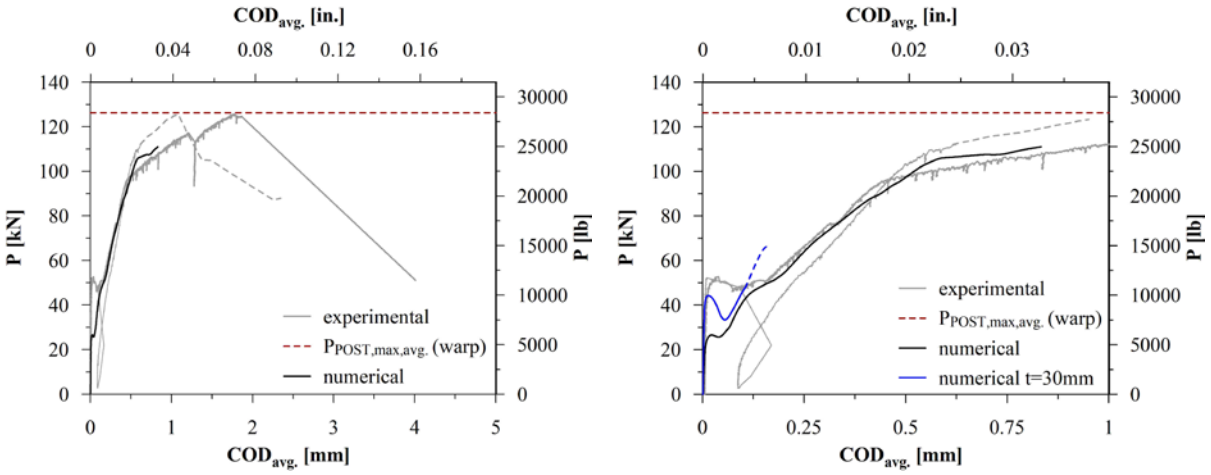

(a) (b)

Fig. 18– Comparison between the experimental and the numerical results for the pre-cracked (PRE) specimens retrofitted with warp-oriented FRCM: global curves (a) and detail in the COD range 0-1 mm (b).

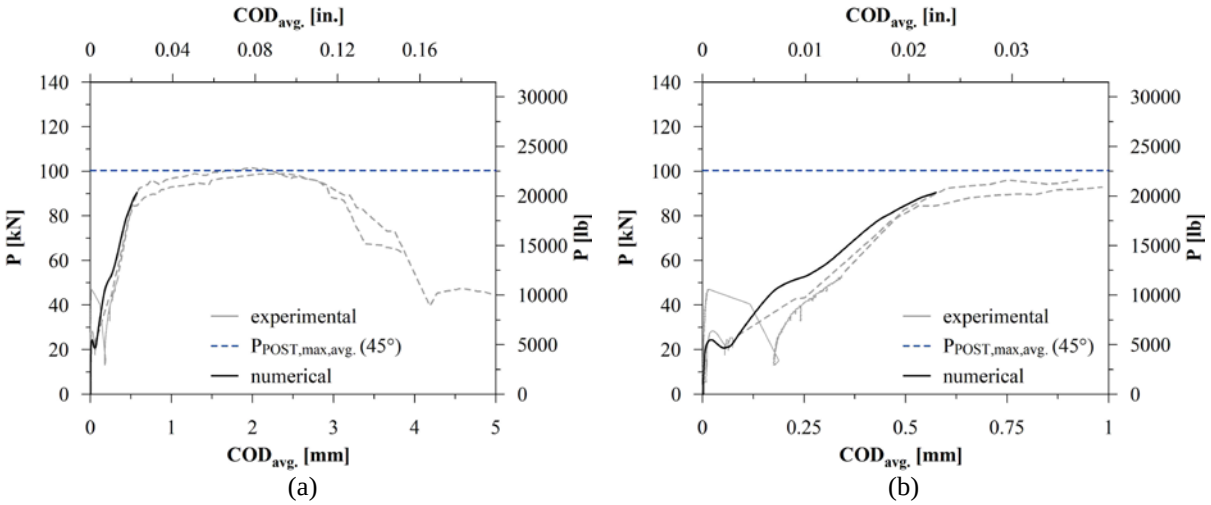

(a) (b)

Fig. 19– Comparison between the experimental and the numerical results for the pre-cracked (PRE) specimens retrofitted with 45°-oriented FRCM: global curves (a) and detail in the COD range 0-1 mm (b).

In all the three models, it can be noticed that the numerical splitting forces at the first cracking are lower than the experimental ones. This is due to the fact that the numerical thickness of the reinforcing layers was taken equal to the nominal one, while in the real application these values were greater due to the hydro-scarification of the substrate concrete. In order to verify this hypothesis, a numerical analysis was performed, doubling the numerical thickness of the composite. From the comparison, shown in **Fig. 18b**, it is possible to appreciate the better correlation reached between numerical and experimental curves in the first cracking phase. Please note that the analysis was interrupted, since the main objective was to compare the responses only at the first cracking stage.

CONCLUSIONS

Based on the experimental evidence, it is possible to draw some conclusions: i) FRCM composites are a promising solution to strengthen and retrofit under-reinforced concrete elements subjected to tensile actions; ii) a proper preparation of the substrate ensures the exploitation of the entire composite capacity, preventing delamination phenomena; iii) the presence of a pre-existing crack in the substrate does not considerably affect the sustained peak load obtained by means of the FRCM layer application, possibly due to the presence of a strong notch in the DEWS sample; and iv) even though the enhancement of the capacity due to a 45° inclined textile is lower with respect to the 0° (warp) one, the solution seems to result in a better control of the cracking process and an increase of the global ductility.

After a preliminary calibration of the numerical models, non-linear analyses targeting FRCM-reinforced concrete members reproduce with a good level of accuracy the experimental results and allow to identify the inelastic process zones. The ultimate capacity is not perfectly captured due to severe strain localizations related to the lack of a bond-slip law at fabric-to-mortar interface; however, the numerical estimation remains on the safe side.

The next phase of the research will comprise the experimental investigation of the effect of different fabric orientations in the FRCM system and, in such cases, the assessment of the effectiveness of the discussed modeling approaches. The final goal will be the simulation of the response of full-scale structural elements characterized by more complex load configurations and reinforcing layouts.

ACKNOWLEDGMENTS

The authors would like to acknowledge Gavazzi Tessuti Spa and BASF Italia Spa for their precious contribution to the research. The research was financially supported by RELUIS WP14 – 2019/2021.

REFERENCES

[1] M. C. Rampini, G. Zani, M. Colombo, and M. di Prisco, “Mechanical Behaviour of TRC Composites: Experimental and Analytical Approaches,” *Appl. Sci.*, vol. 9, no. 7, p. 1492, 2019.

[2] A. Peled, A. Bentur, and B. Mobasher, *Textile reinforced concrete*, 1st ed. Boca Raton, FL, USA: CRC Press, 2017.

[3] W. Brameshuber, Ed., “State-of-the-Art report of RILEM Technical Committee TC 201-TRC ‘Textile Reinforced Concrete,’” 2006.

[4] L. N. Koutas, Z. Tetta, D. A. Bournas, and T. C. Triantafillou, “Strengthening of Concrete Structures with Textile Reinforced Mortars: State-of-the-Art Review,” *J. Compos. Constr.*, vol. 23, no. 1, p. 03118001, 2018.

[5] O. Awani, T. El-Maaddawy, and N. Ismail, “Fabric-reinforced cementitious matrix: A promising strengthening technique for concrete structures,” *Constr. Build. Mater.*, vol. 132, pp. 94–111, 2017.

[6] S. Scheerer, R. Zobel, E. Müller, T. Senckpiel-Peters, A. Schmidt, and M. Curbach, “Flexural strengthening of rc structures with TRC-experimental observations, design approach and application,” *Appl. Sci.*, vol. 9, no. 7, 2019.

[7] M. Herbrand, V. Adam, M. Classen, D. Kueres, and J. Hegger, “Strengthening of Existing Bridge Structures for Shear and Bending with Carbon Textile-Reinforced Mortar,” *Materials (Basel).*, vol. 10, no. 9, 2017.

[8] A. Brückner, R. Ortlepp, and M. Curbach, “Textile reinforced concrete for strengthening in bending and shear,” *Mater. Struct. Constr.*, vol. 39, no. 8, pp. 741–748, 2006.

[9] S. De Santis and G. De Felice, “Tensile behaviour of mortar-based composites for externally bonded reinforcement systems,” *Compos. Part B Eng.*, vol. 68, pp. 401–413, 2015.

[10] L. Anania, A. Badalà, and G. D’Agata, “Numerical simulation of tests for the evaluation of the performance of the reinforced concrete slabs strengthening by FRCM,” *Curved Layer. Struct.*, vol. 3, no. 1, pp. 63–73, 2016.

[11] K. Georgiadi-Stefanidi, E. Mistakidis, P. Perdikaris, and T. Papatheocharis, “Numerical simulation of tested reinforced concrete beams strengthened by thin fibre-reinforced cementitious matrix jackets,” *Earthq. Struct.*, vol. 1, no. 4, pp. 345–370, Dec. 2010.
[12] CEB-FIP, *Model Code 2010 - Volume 1*. 2010.
[13] UNI EN 196, “Method of Testing Cement-Part 1: Determination of Strength.” UNI EN: Brussels, Belgium, 2005.
[14] I. 4606, “Textile Glass—Woven Fabric—Determination of Tensile Breaking Force and Elongation at Break by the Strip Method.” Geneva, Switzerland, 1995.
[15] M. C. Rampini, G. Zani, M. Colombo, and M. Di Prisco, “Textile reinforced concrete composites for existing structures: Performance optimization via mechanical characterization,” in *Proceedings of the 12th fib International PhD Symposium in Civil Engineering*, 2018, pp. 1–8.
[16] J. Aveston and A. Kelly, “Theory of multiple fracture of fibrous composites,” *J. Mater. Sci.*, vol. 8, no. 3, pp. 352–362, 1973.
[17] H. Cuypers and J. Wastiels, “Stochastic matrix-cracking model for textile reinforced cementitious composites under tensile loading,” *Mater. Struct. Constr.*, vol. 39, no. 292, pp. 777–786, 2006.
[18] M. di Prisco, L. Ferrara, and M. G. L. Lamperti, “Double edge wedge splitting (DEWS): An indirect tension test to identify post-cracking behaviour of fibre reinforced cementitious composites,” *Mater. Struct. Constr.*, vol. 46, no. 11, pp. 1893–1918, 2013.
[19] E. Brühwiler and F. H. Wittmann, “The wedge splitting test, a new method of performing stable fracture mechanics tests,” *Eng. Fract. Mech.*, vol. 35, no. 1–3, pp. 117–125, 1990.
[20] A. Magri, M. Colombo, and M. di Prisco, “TRM and UHPFRC: Retrofitting solutions for structural elements.,” in *Proc., Concrete Repair, Rehabilitation and Retrofitting III – Proceedings oft he 3rd ICCRRR*, 2012, pp. 1292-1297.
[21] J. Lee and G. L. Fenves, “Plastic-damage model for cyclic loading of concrete structures,” *J. Eng. Mech.*, vol. 124, no. 8, pp. 892–900, 1998.
[22] Simulia, “Abaqus Analysis User’s Guide.” 2014.
[23] A. Demir, H. Ozturk, K. Edip, M. Stojmanovska, and A. Bogdanovic, “Effect of Viscosity Parameter on the Numerical Simulation of Reinforced Concrete Deep Beam Behavior,” *Online J. Sci. Technol.*, vol. 8, no. 3, pp. 50–56, 2018.

Marco Carlo Rampini is PhD candidate in Structural, Seismic and Geotechnical Engineering at Politecnico di Milano. He received his master's degree in Civil Engineering from Politecnico di Milano. His research interests are the mechanical characterization of fabric-reinforced cementitious matrix composites and the study of their application in strengthening and retrofitting of concrete and masonry structures.

Giulio Zani is a Postdoctoral Research Fellow at Politecnico di Milano. He received both his MS in Architectural Engineering and his PhD in Structural, Seismic and Geotechnical Engineering from Politecnico di Milano. His research interests include the mechanical characterization and the structural application of fiber-reinforced and textile-reinforced cement-based composites.

Matteo Colombo is an Associate Professor at Politecnico di Milano (Department of Civil and Environmental Engineering). He has taken part in several national and international research projects. His research interests include the investigation on mechanical behaviour and on structural applications of advanced cementitious composites (fibre reinforced concrete and textile reinforced concrete) in standard and extreme conditions (e.g. fire and blast).

Marco di Prisco is a Professor of Structural Design at Politecnico di Milano. Honorary Editor of the European Journal of Environmental and Civil Engineering, member of the Editorial Board of the Journal of Cement and Concrete Composites, member of fib presidium, he is the convener of the Commission TC250/SC2/Wg1/Tg2 to introduce FRC in EC2. His research interests include composite cement-based materials, fracture mechanics, reinforcement-concrete interaction, r/c and p/c structural elements, prefabricated structures, structural response at exceptional loads.